

Cell Reports, Volume 33

Supplemental Information

USP15 Deubiquitinase Safeguards

Hematopoiesis and Genome Integrity

in Hematopoietic Stem Cells and Leukemia Cells

Paul van den Berk, Cesare Lancini, Carlos Company, Michela Serresi, Maria Pilar Sanchez-Bailon, Danielle Hulsman, Colin Pritchard, Ji-Ying Song, Matthias Jürgen Schmitt, Ellen Tanger, Oliver Popp, Philipp Mertins, Ivo J. Huijbers, Heinz Jacobs, Maarten van Lohuizen, Gaetano Gargiulo, and Elisabetta Citterio

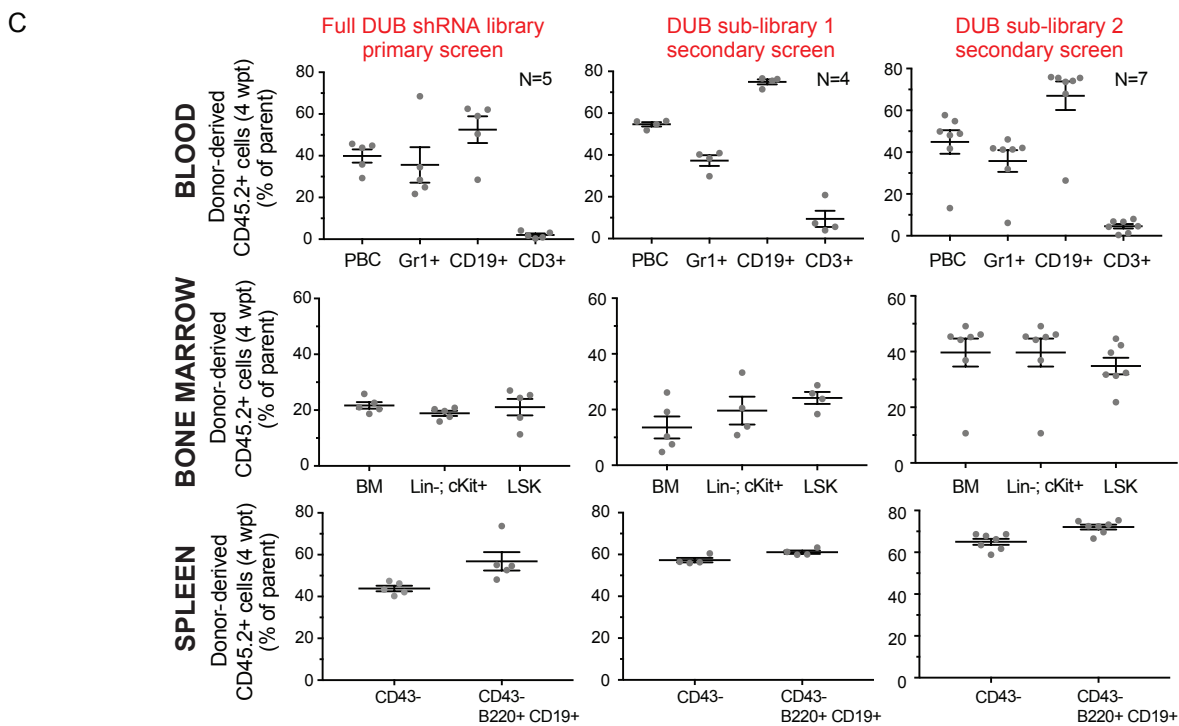
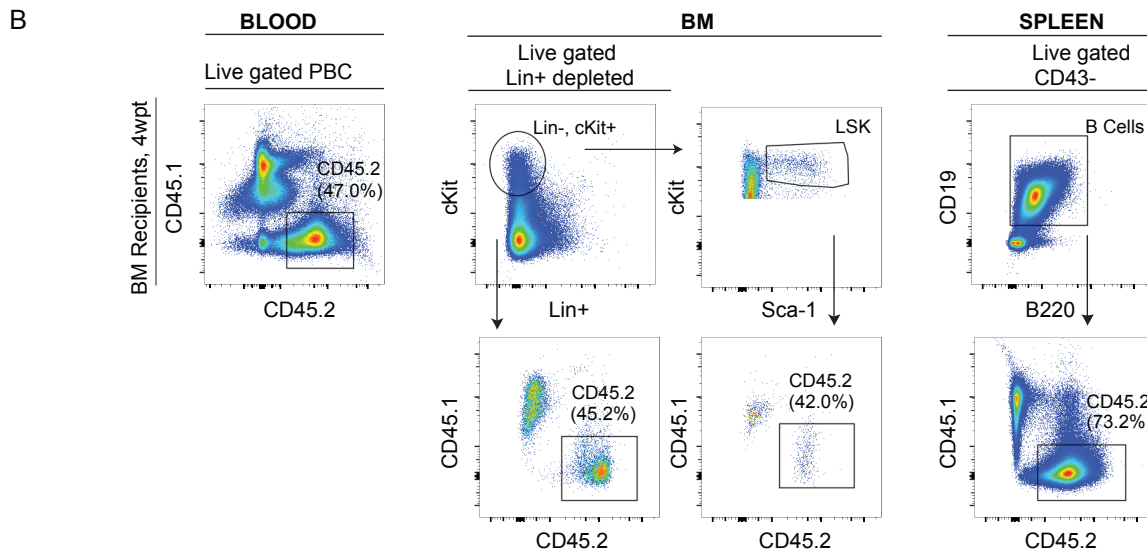
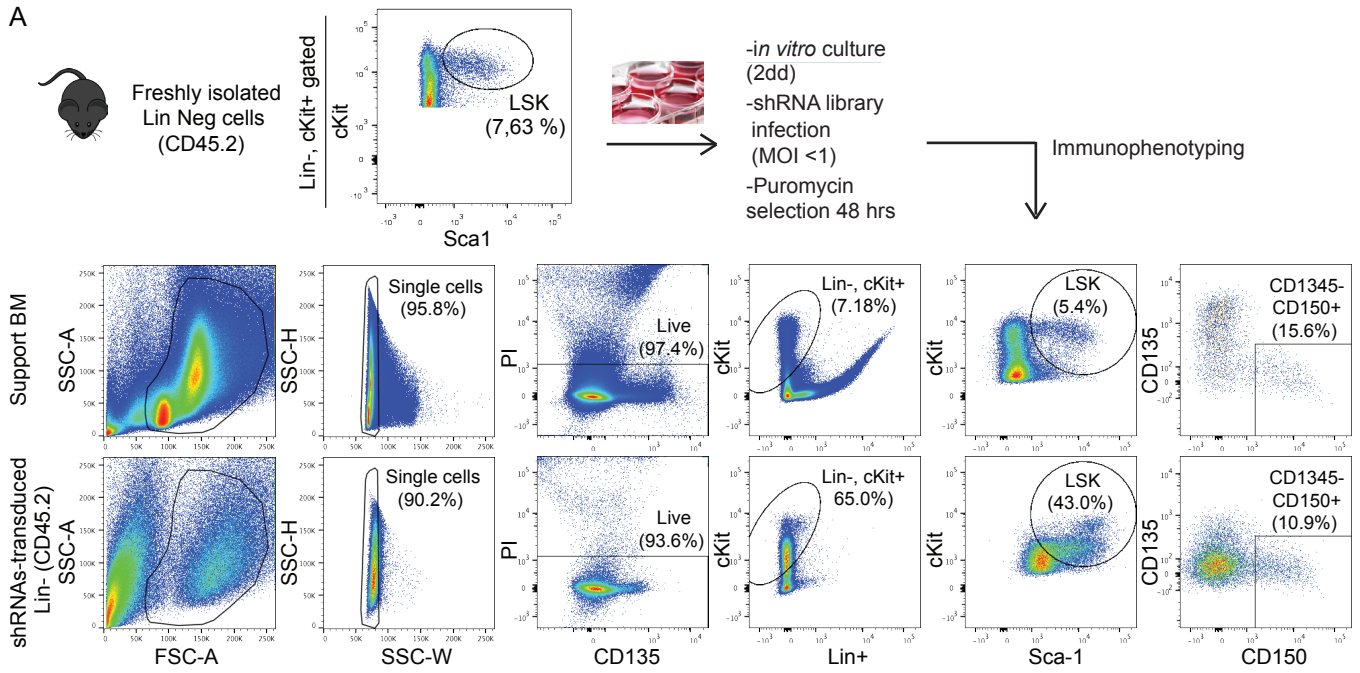


Figure S1. *In vivo* RNAi screens for DUBs in murine hematopoietic stem and progenitor cells, Related to Figure 1.

Figure S1. *In vivo* RNAi screens for DUBs in murine hematopoietic stem and progenitor cells, Related to Figure 1.

(A) Early progenitors (LSK) population is enriched and it is retained upon viral transduction *in vitro*. Lineage negative (Lin⁻) cells isolated from wt (CD45.2) bone marrow (BM) were grown under stem cell conditions and transduced with pooled shRNA lentiviral libraries targeting all annotated mouse orthologues of human DUBs. After selection, CD45.2 transduced Lin⁻ cells are mixed 1:1 with CD45.1 support BM cells. Top panel: representative FACS profiles and relative percentage of LSK (Lin⁻ Sca1⁺ cKit⁺) cells in freshly isolated Lin⁻, cKit^{high} progenitors. Middle and lower panels: gating strategy and FACS profiles for BM cell subsets in support BM (middle panel) and in shRNA library-transduced Lin⁻ cells prior transplantation (lower panel). LSK were gated on the basis of CD135/Flk-2 and SLAMF7/CD150 surface markers to assess immature precursors endowed with reconstitution potential (LSK, CD135⁻, CD150⁺) (Christensen and Weissman, 2001; Kiel et al., 2005; Yeung and Wai Eric So, 2009). Frequency in the parental cell population is shown.

(B-C) ShRNA library-transduced Lin⁻ cells efficiently engraft and contribute to BM repopulation (4 wpt). Representative FACS profiles (B) and quantification of engraftment for each screen (C) (primary screen, left panels; secondary screens, middle and right panels) is shown. Total reconstitution of peripheral blood cells (PBC) and contribution of donor-derived, transduced (CD45.2) Lin⁻ cells to Gr1⁺, CD19⁺ (B cells) and CD3⁺ (T cells) in the blood (C, upper panels), BM (total BM cells, Lin⁻, cKit⁺ cells and LSK cells) (C, middle panels), and to splenic CD43⁻ and B cells (CD43⁻, CD19⁺, CD220⁺) (C, bottom panels) in recipient mice at 4 wpt is shown. Error bars represent \pm SEM.

For isolation of resting B cells from spleen single cell suspension, CD43 positive cells were first depleted using anti-mouse CD43 (Ly-48). Donor-derived cells were then phenotypically analyzed and isolated by FACS sorting using fluorochrome-labeled antibodies.

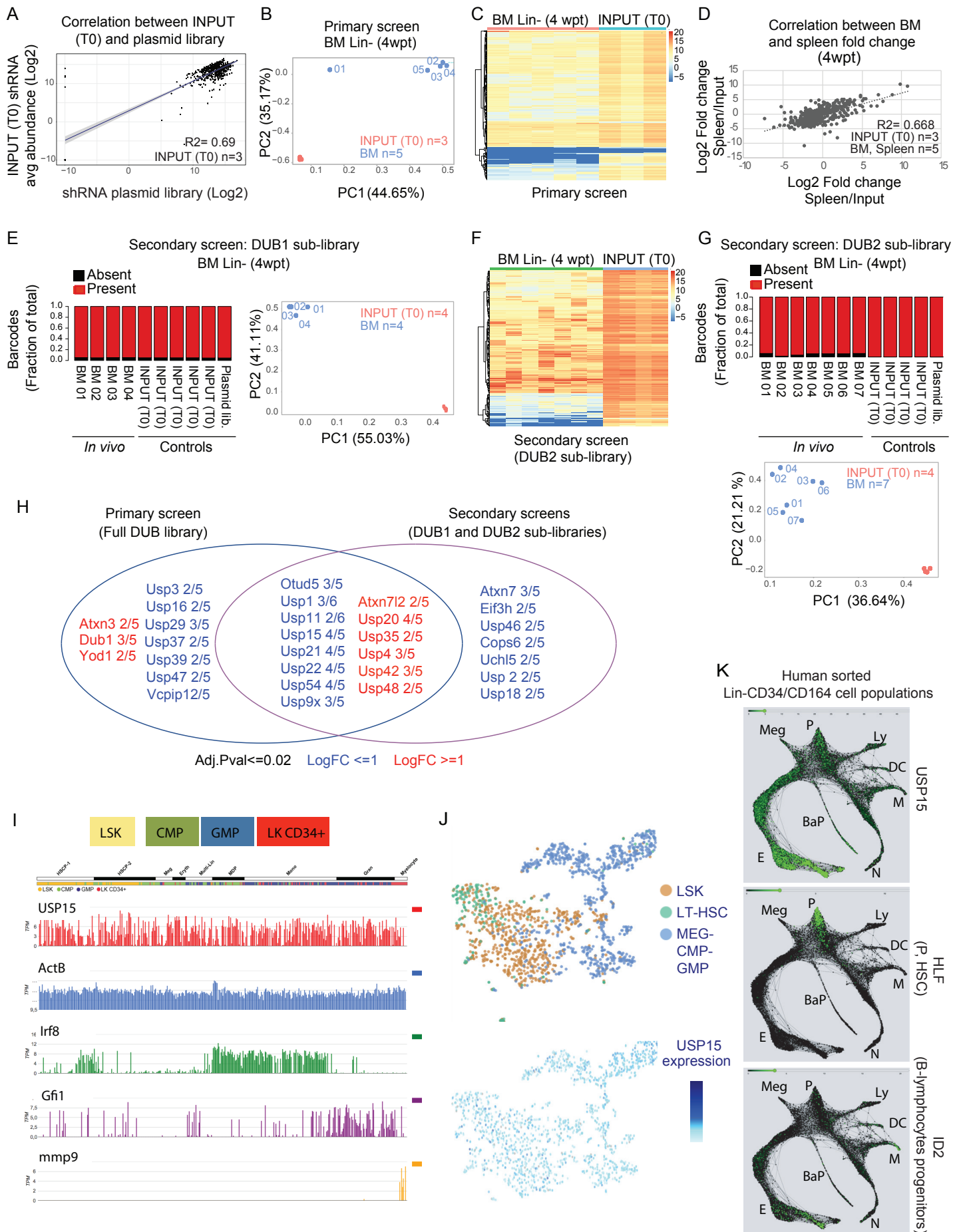


Figure S2. Pooled *in vivo* RNAi screens identify candidates DUBs effectors of HSC activity, Related to Figure 1.

Figure S2. Pooled *in vivo* RNAi screens identify candidates DUBs effectors of HSC activity, Related to Figure 1.

(A-D) Primary screen, full DUB library.

(A) shRNAs library complexity is maintained in transduced Lin⁻ cells. Pairwise correlation between the shRNA-seq profiles of the plasmid DNA (plasmid library) used to generate the viral pool and the genomic DNA isolated from Lin⁻ cells infected with the same viral pool prior transplantation, INPUT (T0).

(B) PC analysis of *in vivo* Lin⁻ cells harvested from recipient mice at 4 wpt and INPUT (T0) samples.

(C) Quantitative heat map depiction of the primary screen with individual shRNAs (in rows) in each replicate (column) shown in red for the highest number of reads and in blue for lowest numbers of reads.

(D) Scatter plot of the change in shRNA representation after *in vivo* growth shows good correlation between the BM and the spleen compared to the input. Person's *r* is indicated.

(E) Secondary screen: DUB1 sub-library. Left panel: consolidated fraction of shRNAs retrieved *in vivo* in BM Lin⁻ cells at 4 wpt and in controls. Right panel: PC analysis of *in vivo* and INPUT (T0) samples.

(F) Quantitative heat map depiction of the secondary screen (DUB2 sub-library) with individual shRNAs (in rows) in each replicate (column) shown in red for the highest number of reads and in blue for lowest numbers of reads.

(G) Secondary screen: DUB2 sub-library. Upper panel: consolidated fraction of shRNAs retrieved *in vivo* in BM Lin⁻ cells at 4 wpt and in controls. Lower panel: PC analysis of *in vivo* and INPUT (T0) samples.

(H) Classification of screen results depicting significantly differentially represented DUBs overlapping between the primary and secondary screens. Candidate genes targeted by at least two shRNAs were selected with the indicated criteria. Genes were not scored if multiple cognate hairpins showed opposing effects. The number of differentially represented shRNAs per gene is indicated.

(I-K) USP15 is highly and homogeneously expressed in the hematopoietic lineage tree at single cell level.

(I) scRNA-Seq on stem/multipotent progenitors (LSK; lin⁻Sca1+c-Kit⁺), common myeloid progenitors (CMP), granulocyte monocyte progenitors (GMP), and LK CD34⁺ cells (lin⁻c-Kit⁺CD34⁺) that included granulocytic precursors. HSCP-1, hematopoietic stem cell progenitor; HSCP-2; Meg, megakaryocytic; Eryth, erythrocytic; Multi-Lin*, multi-lineage primed; MDP, monocyte-dendritic cell precursor; Mono, monocytic; Gran, granulocytic; and myelocyte, myelocytes and metamyelocytes. EndFragment. Mouse Expression (Olsson et al., 2016).

(J) scRNA-seq on HSC/hematopoietic progenitors. LSK, hematopoietic stem cells and hematopoietic multipotent progenitors; LT-HSC, long-term hematopoietic stem cells (Lin⁻c-Kit⁺Sca1+CD34⁻Flk2⁻); MEP-CMP-GMP, megakaryocyte-erythroid progenitor cells (MEP), common myeloid progenitors (CMP), and granulocyte-monocyte progenitors. Mouse Expression (Nestorowa et al., 2016).

(K) USP15 is expressed in single cells human CD34⁺ HSC and progenitors.

Analysis of USP15 expression in scRNA-seq data set of the human Lin⁻compartment, as investigated by means of CD34/CD164 fractionation (Pellin et al., 2019). The panels represent a SPRING plot of sorted human Lin⁻CD34/CD164 single-cell transcriptomes. Each point is one cell. Labels at the edges represent the transcriptional states associated to early lineage commitment

(P, early progenitor cells; Meg, megakaryocytes; E, erythroid cells; BaP, basophilprogenitors; N, neutrophils; M, monocytes; DC, dendritic cells; Ly-T/B/NK, lymphoid T/B/NK cells) (Pellin et al., 2019). Plots of USP15 expression and of the lineage defining genes HLF (P, HSC) and ID2 (B-lymphocytes progenitors branch) (LRT adjusted pvalue < 0.05) is shown in each panel.

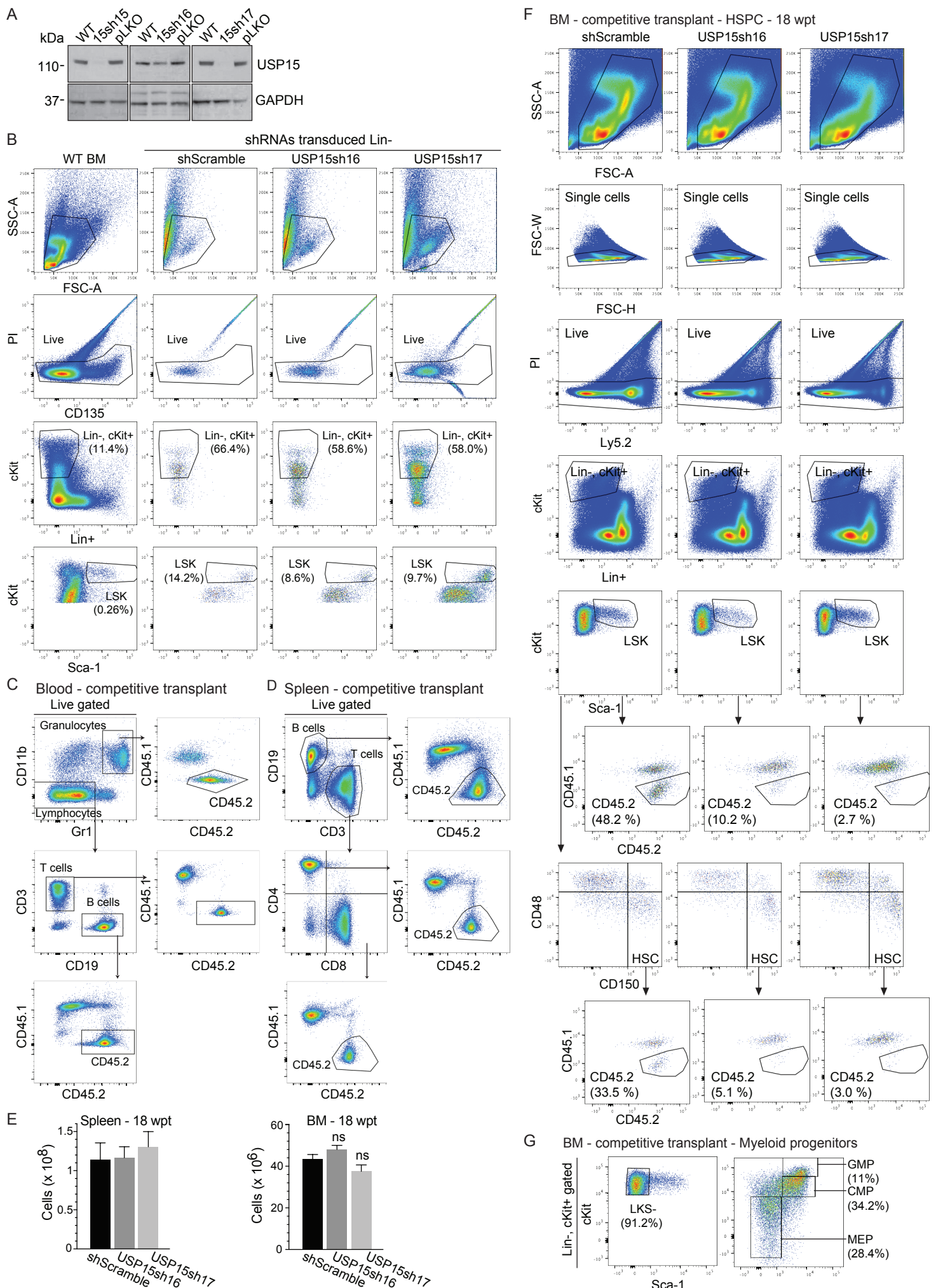


Figure S3. Hairpin validation, flow cytometry analysis and gating strategies for BM transplantation assays, Related to Figure 2 and Figure 4A, B.

Figure S3. Hairpin validation, flow cytometry analysis and gating strategies for BM transplantation assays, Related to Figure 2 and Figure 4A, B.

(A) Wild type (WT) KPE primary mouse NSCLC cells (Serresi et al., 2016) were infected with empty lentiviral vector (pLKO) or USP15-targeting (shUSP15) shRNAs expressing lentiviruses and puromycin-selected for 48hrs. The knockdown efficiency of USP15 was detected by immunoblot. Related to Figure 2B.

(B) Flow cytometry analysis of Lin⁻ cells transduced with the indicated shRNA and grown *in vitro*. Full FACS representative profiles and frequency of Lin⁻, cKit⁺ and of LSK per live cells are shown (related to Figure 2C).

(C, D) Gating strategy for blood and spleen subsets analysis in bone marrow transplantation assays (related to Figure 2E-G and to Figure 4A, B).

(E-G) Freshly isolated wt murine Lin⁻ cells were transduced with shRNAs targeting USP15 or control shRNA and assayed in competitive bone marrow transplantation.

(E) Total number of cells in the bone marrow (BM, left panel) and in the spleen (right panel) of recipient mice at 18 wpt is shown (related to Figure 2G and 2H-K).

P-value was assessed by Student's t test in Prism 7. ns, non significant. Data represent mean values \pm SEM. N=3 per shRNA, except for shUSP15#16, n=4.

(F) Full gating strategy and representative FACS profiles for hematopoietic stem and progenitor compartment analysis (related to Figure 2H-J). Within the lineage⁻, Sca1⁺, c-Kit⁺ (LSK) population, cells were gated based on CD48 and CD150 to identify HSC (Cabezas-Wallscheid et al., 2014; Kiel et al., 2005). Percentages of the CD45.2 positive cells in the parental cell populations (LSK) or (HSC) are shown.

(G) Gating strategy for myeloid progenitors (related to Figure 2K). Within the lineage⁻, c-Kit⁺, Sca1⁻ (LKS⁻) population, cells were gated based on CD16/32 and CD34 expression to identify common myeloid progenitors (CMP), granulocyte monocyte progenitors (GMP) and megakaryocyte erythrocyte progenitors (MEP). Frequency in the parental cell populations is shown.

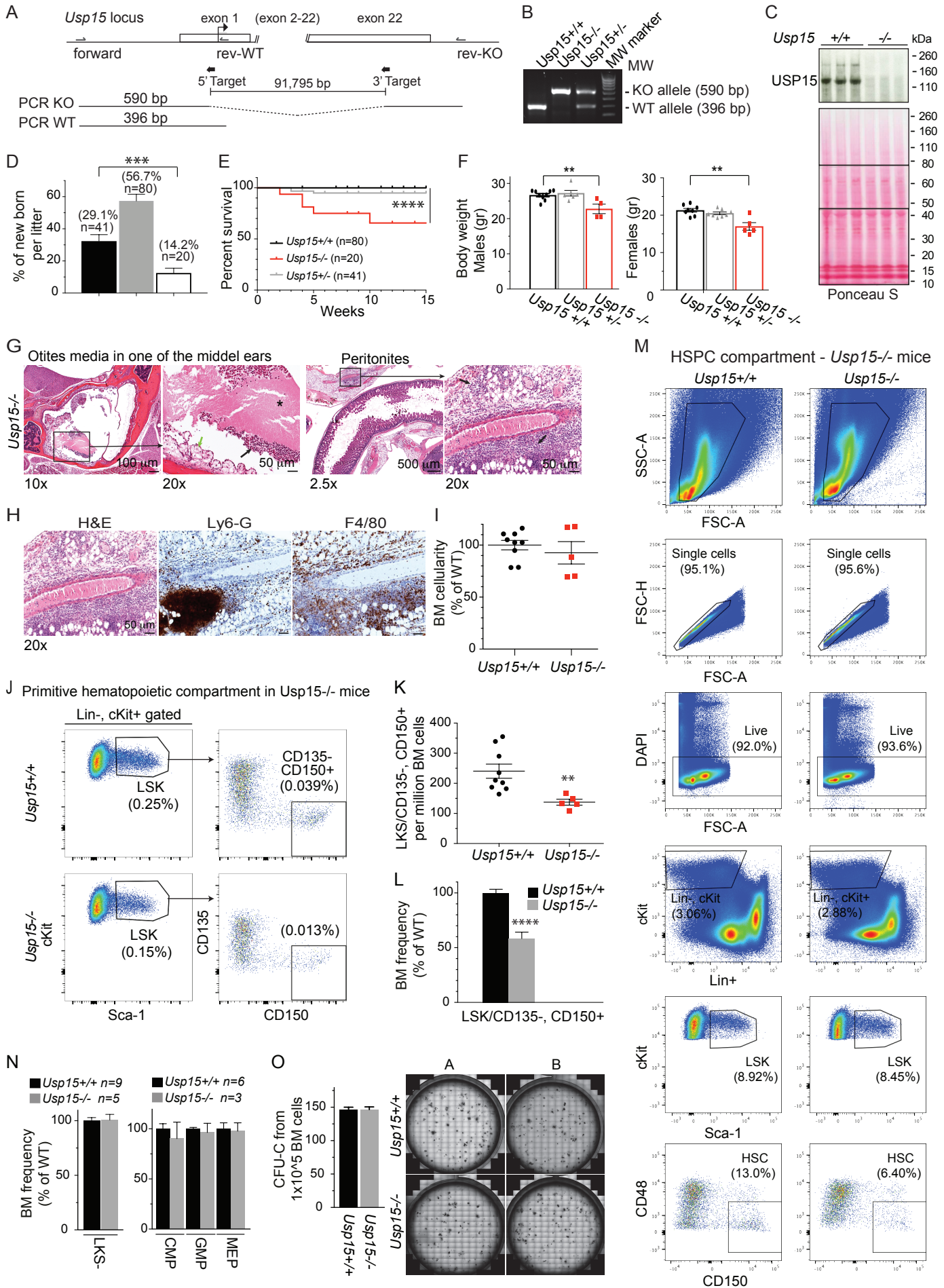


Figure S4. Generation and initial characterization of *Usp15* knockout mouse model, Related to Figure 3.

Figure S4. Generation and initial characterization of *Usp15* knockout mouse model, Related to Figure 3.

(A) Schematic representation of the strategy for germline deletion of the entire mouse *Usp15* locus (91,795 bp) by CRISPR/Cas9. On top: wild-type *Usp15* genomic locus. Oligos (arrows) for PCR screening are indicated. Middle: targeting primers positioned at the transcriptional start site within exon 1 (5' Target) and after the PolyA signal in exon 22 (3' Target). Bottom: PCR fragments corresponding to the *Usp15* knockout (KO) or wild-type (wt) allele.

(B) PCR analysis of genomic tail tip DNA.

(C) Immunoblot of whole cell extract from freshly isolated BM cells from *Usp15*^{+/+} (n=3) and *Usp15*^{-/-} (n=3) mice with anti-USP15 antibody. Total proteins staining with Ponceau S is shown (lower panel).

(D) Genotype frequency per litter, on a total of 31 litters. n = number of born mice/genotype.

(E) Kaplan-Meier survival analysis.

(F) Body weight of mice of the indicated genotype. Males, 8-12 wks old. Females, 8-14 wks old.

(G) Histopathological analysis of *Usp15*^{-/-} mice. Full pathological analysis was performed on 6 *Usp15*^{+/+} and 5 *Usp15*^{-/-} mice between 10 and 12 weeks of age. 3 out of 5 *Usp15*^{-/-} animals showed inflammatory lesions, in one case severe (bottom). Top: representative H&E-stained head from a *Usp15*^{-/-} mouse (11 wks) showing lesions of otitis media in one of the inner ears. Proteaceous material (*) with dead cells and inflammatory cells (black arrow) is visible, as well as edema (green arrow). Bottom: Representative H&E-stained intestine from a *Usp15*^{-/-} mouse (11 wks) showing severe inflammatory lesions with massive immune cells infiltration in the mesentery (black arrows). No lesions were found in *Usp15*^{+/+} littermates (not shown).

(H) Immunohistochemistry (IHC) of Ly6-G and F4/80 confirmed the nature of multiple inflammatory lesions encountered in the skin and abdominal cavity of the mouse (case n.1 in Table S7). As shown in the representative microphotographs of mesentery stained by H&E (Hematoxylin/Eosin) and IHC, the cells involved in the massive inflammatory infiltrations were mainly those neutrophils and macrophages that were labeled by Ly6-G and F4/80, respectively. The inflammation was accompanied by multiple necrotic changes. Thereby a nature of acute purulent inflammation is evident. Bar: 50 μ m.

(I) Bone marrow was isolated from femurs of *Usp15*^{+/+} (n=9) and *Usp15*^{-/-} (n=5) 8-12 wks old mice. The number of total BM live cells was calculated and normalized to *Usp15*^{+/+} littermates.

(J-O) Hematopoietic primitive compartment in USP15 knockout mice (relative to Figure 4).

(J-N) Multiparameter flow cytometry analysis of the hematopoietic primitive populations in *Usp15*^{+/+} and *Usp15*^{-/-} mice (8-12 wks old).

(J) Gating strategy with representative FACS profiles using CD135/Flk-2 and CD150 surface markers to assess immature precursors endowed with reconstitution potential (LSK, CD135-, CD150+)(Christensen and Weissman, 2001; Kiel et al., 2005; Yeung and Wai Eric So, 2009).

(K) LSK, CD150+, CD135- cell numbers per million live BM cells.

(L) Frequency of LSK, CD150+, CD135- immature precursors in bone marrow of *Usp15*^{-/-} mice was calculated and normalized to *Usp15*^{+/+} animals (*Usp15*^{+/+} n=9, *Usp15*^{-/-} n=5).

(M) Flow cytometry analysis and representative FACS profiles for hematopoietic stem and progenitor compartment in 8-12 wks old *Usp15*^{+/+} and *Usp15*^{-/-} mice (related to Fig. 3).

(N) BM frequency of the indicated progenitor populations in *Usp15*^{-/-} mice normalized to *Usp15*^{+/+} animals. Results are from three (K, L, and M left panel) (*Usp15*^{+/+} n=9, *Usp15*^{-/-} n=5) or two (M, right panel) independent experiments.

(O) BM cells from wt or *Usp15*^{-/-} mice were assayed for myeloid colony-forming (CFU-C) ability. Results are the mean \pm SEM from two independent experiments, $n = 3$ per genotype per experiment. Representative images of two technical replica (A, B) are shown. For all panels: **, $P \leq 0.01$; ***, $P \leq 0.001$; ****, $P \leq 0.0001$. P-value was assessed by Student's t test (D, F, K, L) or by Log-rank test (E). Mean \pm SEM is shown.

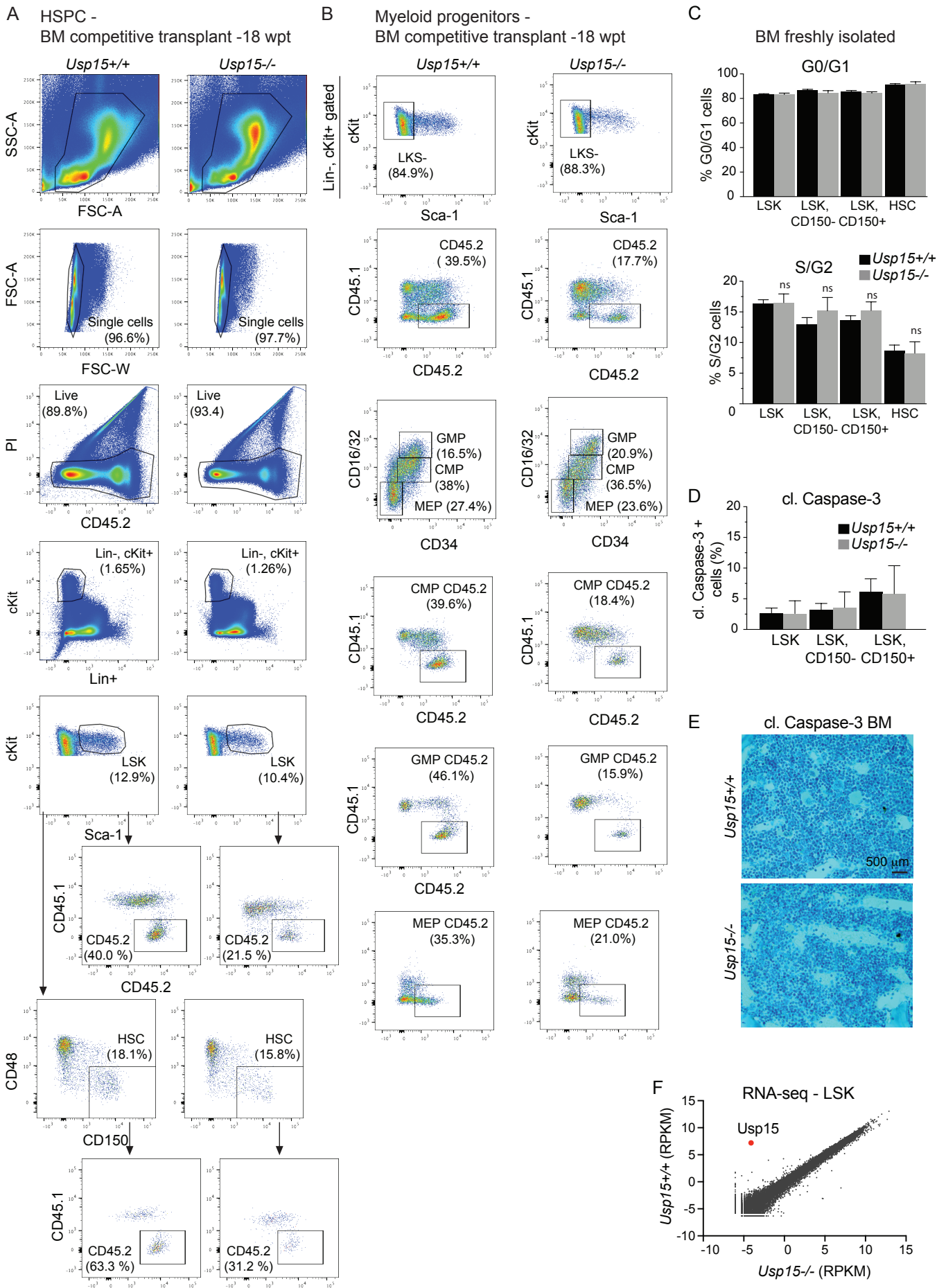


Figure S5. BM transplantation and *Usp15^{+/+}* and *Usp15^{-/-}* mice hematopoiesis, Related to Figure 4.

Figure S5. BM transplantation and *Usp15*^{+/+} and *Usp15*^{-/-} mice hematopoiesis, Related to Figure 4.

(A, B) BM analysis, HSPC subsets (A) and myeloid progenitors (B) in competitive BM transplantation primary recipient mice at 18 wpt (related to Fig. 4). Frequency in the parental cell populations is shown.

(C) Cell cycle analysis of hematopoietic stem and progenitor cells populations in wt and USP15 knockout mice. Percentage of G0/G1 and S/G2 cells in *Usp15*^{+/+} and *Usp15*^{-/-} mice was determined by DAPI analysis in 12-16 weeks old mice. *Usp15*^{+/+}, n=10; *Usp15*^{-/-}, n=5. Results are the mean ± SEM of three independent experiments.

(D) Cleaved (cl.) Caspase-3 analysis of freshly isolated hematopoietic stem and progenitor cells in *Usp15*^{+/+} and *Usp15*^{-/-} mice. Results are the mean ± SEM of two independent experiments. *Usp15*^{+/+}, n=6; *Usp15*^{-/-}, n=2. 15-20 weeks old mice.

(E) Representative images of *Usp15*^{+/+} and *Usp15*^{-/-} BM sections stained for apoptosis-indicating cleavage (cl.) of Caspase-3. *n* = 6 mice per genotype. Bar, 500 μm.

(F) RNA-seq of LSK population freshly isolated from BM. Comparison of normalized gene expression data for *Usp15*^{-/-} (n=2) versus *Usp15*^{+/+} (n=3) LSK (2 months old mice). USP15 expression is highlighted in red.

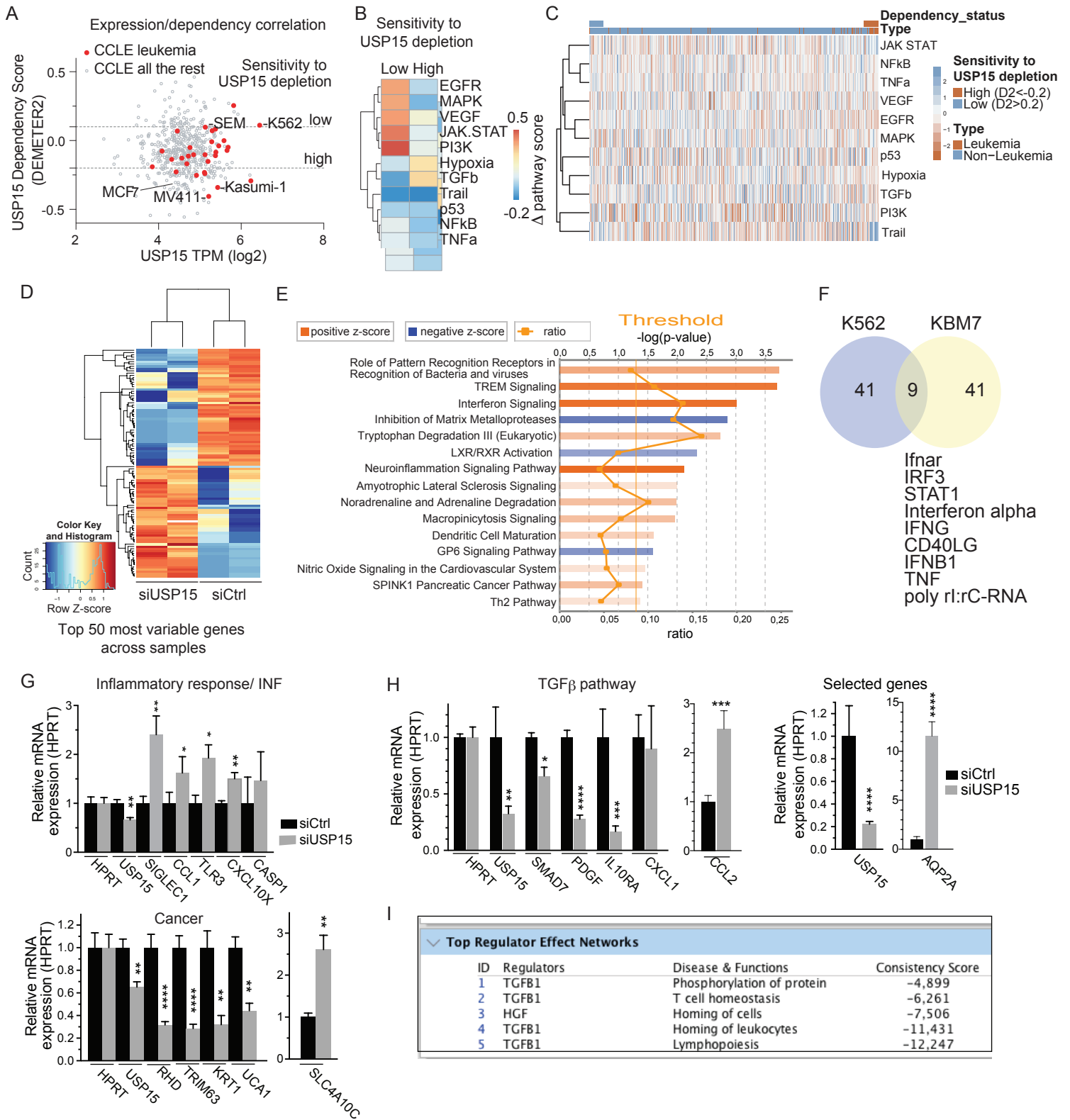


Figure S6. USP15 RNAi in CML cell lines results in alteration of inflammatory signaling pathways, Related to Figure 5.

Figure S6. USP15 RNAi in CML cell lines results in alteration of inflammatory signaling pathways, Related to Figure 5.

(A) The dependency scores were calculated by Demeter2 for USP15 RNAi in CCLE lines (McFarland et al., 2018) and correlated to USP15 gene expression levels. TPM (Transcripts Per Million).

(B) Differential pathway activation by PROGENy for cell lines with DEMETER2 scores $D2 < -0.2$ (Low) and $D2 > 0.2$ (high).

(C) Heat map showing PROGENy scores for the indicated pathways (rows) in all the CCLE cell lines (columns). Rows are sorted by correlation whereas columns are sorted by DEMETER2 score. The legends indicate DEMETER2 score and tumor type.

(D-I) KBM7 (D, E, F, G) or K562 (F, H, I) cells were transfected with USP15 (siUSP15) or non-targeting (siCtrl) siRNA pool. At 72 hours after transfection, cells were harvested and RNA was extracted and subjected to RNAseq (D, E, F, I) or used for RT-qPCR analysis (G, H).

(D) Unbiased clustering of genes significantly dysregulated (>1 fold change and Adjusted P value < 0.05) in KBM7 RNAseq dataset.

(E) Ingenuity pathway analysis of USP15-dependent genes in the KBM7 dataset showing dysregulated top canonical pathways (cut-off $\log_{2}FC > 1$; adjusted P value < 0.05).

(F) Venn diagram depicting the overlap between Top 50 significantly enriched Ingenuity Upstream Regulators in each cell line RNAseq datasets. The Upstream Regulators were calculated based on differential gene expression between USP15 and control siRNAs. The nine overlapping terms are indicated below.

(G) qRT-PCR analysis of the indicated genes in KBM7 USP15 knock down cells.

(H) qRT-PCR analysis of the indicated genes in K562 USP15 knock down cells.

(I) USP15 RNAi in K562 cells. Ingenuity pathway analysis of USP15-dependent genes in the K562 RNAseq dataset showing dysregulated Top Regulator Effect Networks (cut-off $\log_{2}FC > 1$; adjusted P value < 0.05).

Results are from one (KBM7) or two independent experiments (K562) per cell line. Each experiment $n=2$ per siRNA/ cell line. Results are mean \pm SD (F, G). **. $P \leq 0.01$; ***. $P \leq 0.001$; ****. $P \leq 0.0001$. P-value was assessed by Student's t test.

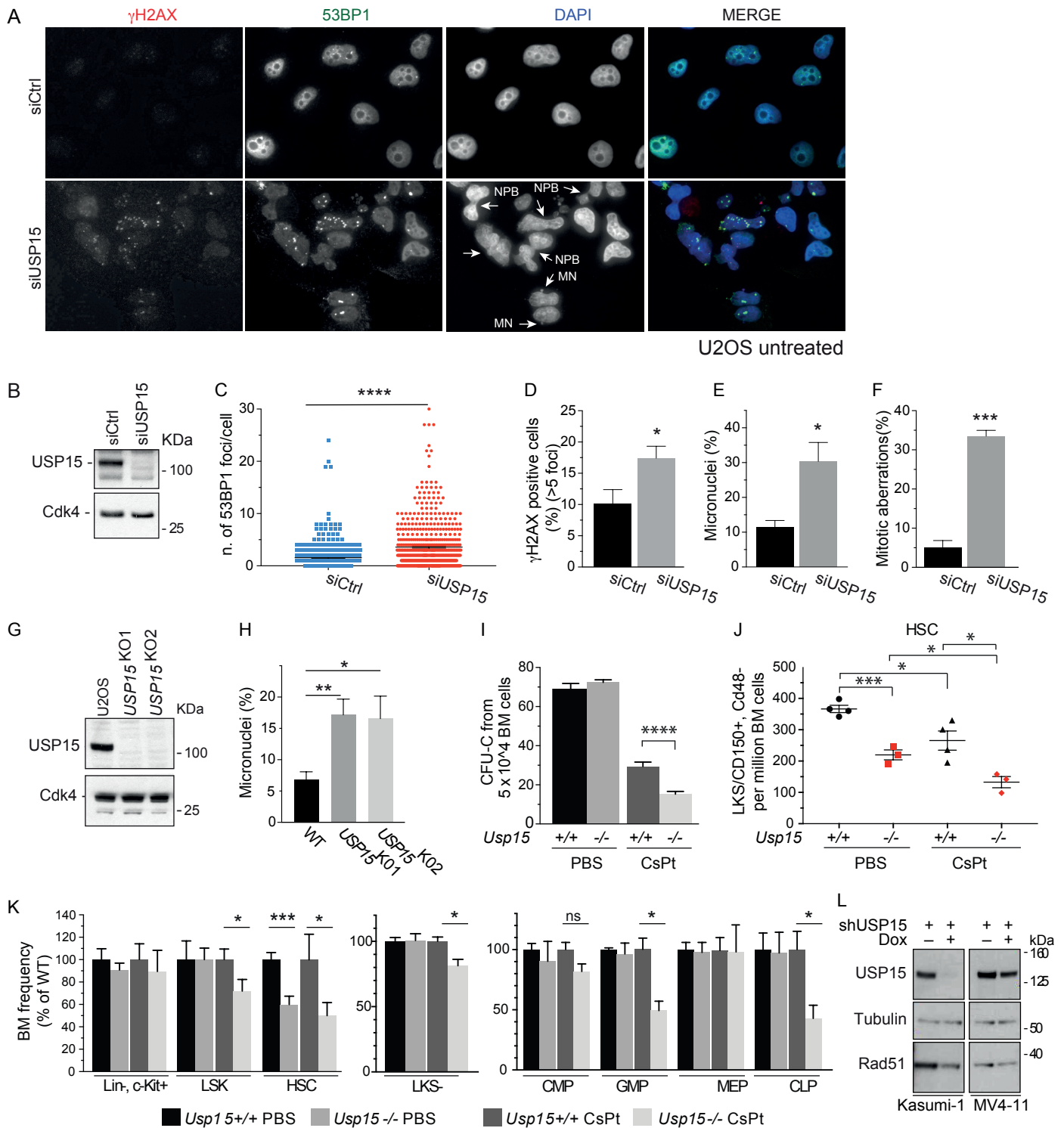


Figure S7. USP15 loss enhances genotoxic stress *in vitro* in human cancer cells and *in vivo* in mouse hematopoietic stem and progenitor cells, Related to Figure 6.

Figure S7. USP15 loss enhances genotoxic stress *in vitro* in human cancer cells and *in vivo* in mouse hematopoietic stem and progenitor cells, Related to Figure 6.

(A-G) Knockdown or CRISPR/Cas9- mediated knockout of USP15 in U2OS cancer cells induces spontaneous DNA damage.

(A-F) U2OS cells were transfected with USP15 (siUSP15) or non-targeting (siCtrl) siRNA pool and assayed at 72 hours after transfection.

(A) Representative images of co-immunostaining for γ H2AX and 53BP1. Arrows indicate micronuclei (MN), nucleoplasmatic bridges (NPB), and abnormal mitosis.

(B) Western blot with the indicated antibodies on whole cell extract.

(C) Quantification by Image J of the number of spontaneous 53BP1 foci per cell. $n=4$ experiments; >400 cells per genotype were in total analyzed. Mean values \pm SEM are shown.

(D) Quantification of the percentage of cells containing >5 spontaneous γ H2AX foci. Mean \pm SD is shown.

(E) Percentage of micronuclei. Mean values \pm SEM are shown.

(F) Percentage of aberrant mitosis, including bi-nucleated cells and cells with nucleoplasmatic bridges. Mean values \pm SEM are shown.

(A-F) All quantifications are from three independent experiments. $n > 50$ cells/genotype/experiment.

(G-H) CRISPR/Cas9- mediated deletion of USP15 in U2OS cells.

(G) Western blot with the indicated antibodies on whole cell extract.

(H) Micronuclei were quantified in wt cells and in two independent USP15 knockout clones, in two independent experiments. A minimum of 100 cells per genotype/clone/experiment were scored. Mean values \pm SEM are shown.

(I-K) USP15 protects the hematopoietic stem and progenitor compartment from genotoxic stress *in vivo*. *Usp15*^{+/+} and *Usp15*^{-/-} mice (8-12 wks old) were injected with PBS or with low dose of cisplatin (CsPt)(0.8 mg/kg i.v.). Mice were sacrificed after 48 hrs.

(I) BM cells were isolated from wt or *Usp15*^{-/-} mice and were assayed for myeloid colony-forming (CFU-C) ability.

(J, K) Multiparameter flow cytometry analysis of the hematopoietic stem and progenitor compartment.

(J) HSC (LSK, CD150+, CD48-) cell numbers per million live BM cells.

(K) The frequency of the indicated cell populations in *Usp15*^{-/-} mice was calculated and normalized to *Usp15*^{+/+} animals. LSK/CD150+ CD48- (HSC), lineage-, c-Kit+, Sca1- (LKS-), common myeloid progenitors (CMP), granulocyte monocyte progenitors (GMP), megakaryocyte erythrocyte progenitors (MEP), common lymphoid progenitors (CLP).

Results are the mean \pm SEM or SD (K, left panel) of two independent experiments. Mice: (J-K) *Usp15*^{+/+} $n = 4$, *Usp15*^{-/-} $n = 3$ per treatment; (K) $n = 3$ per genotype per treatment.

(L) Kasumi-1 and MV4-11 cells harboring USP15 shRNA were kept in medium with or without doxycycline (Dox) for 5 days. Western blot was performed with the indicated antibodies. One representative experiment out of 2 is shown.

For all panels: *, $P \leq 0.05$; **, $P \leq 0.01$; ***, $P \leq 0.001$; ****, $P \leq 0.001$ as assessed by Student's t test.

Table S4. Primer sequences for Illumina sequencing multiplexing strategy, Related to Figure 1.

PCR 1, forward primer	<i>ACACTCTTTCCTACACGACGCTCTCCGATCT</i> <u>NNNNNN</u> GGCTTTATATATCTTGTGGAAA GGACG
PCR 1, reverse primer	GTGACTGGAGTTCAGACGTGTGCTCTCCGATCTGTGGATGAATACTGCCATTTGTCTC
PCR 2, forward primer	AATGATACGGCGACCACCGAGATCT <i>ACACTCTTTCCTACACGACGCTCTCCGATCT</i>
PCR 2, reverse primer	CAAGCAGAAGACGGCATACGAGAT <u>NNNNNN</u> GTGACTGGAGTTCAGACGTGTGCTCTT CCGATCT
PCR 1 barcodes (green)	
Barcode #1	CGTGAT
Barcode #2	ACATCG
Barcode #3	GCCTAA
Barcode #4	TGGTCA
Barcode #5	CACTGT
Barcode #6	ATTGGC
Barcode #7	GATCTG
Barcode #8	TCAAGT
Barcode #9	CTGATC
Barcode #10	AAGCTA
Barcode #11	GTAGCC
Barcode #12	TACAAG
PCR 2 Illumina Indexes (green)	
Index #1	ATCACG
Index #2	CGATGT
Index #3	TTAGGC
Index #4	TGACCA

PCR1 forward primer is designed to include: Illumina/Solexa adapter 1 (red, italics), barcode (green, bold and underlined), pLKO.1 common region (plain text).

Table S5. Hematopoietic stem and progenitor cell populations and their markers, Related to Figures 2, 3 and 4.

Subset	Subpopulations	Markers
Lin ⁻	LSK, HSC, LKS ⁻ , CMP, GMP, MEP	Lineage ⁻
LSK	HSC	Lineage ⁻ , Sca-1 ⁺ , cKit ⁺
HSC		Lineage ⁻ , Sca-1 ⁺ , cKit ⁺ , CD150 ⁺ , CD48 ⁻
LKS ⁻	CMP, GMP, MEP	Lineage ⁻ , Sca-1 ⁻ , cKit ⁺
CMP		Lineage ⁻ , Sca-1 ⁻ , cKit ⁺ , CD34 ^{int} , CD16/32 ^{int}
GMP		Lineage ⁻ , Sca-1 ⁻ , cKit ⁺ , CD34 ⁺ , CD16/32 ⁺
MEP		Lineage ⁻ , Sca-1 ⁻ , cKit ⁺ , CD34 ⁻ , CD16/32 ⁻

Table S6. List of antibodies used in this study, Related to STAR Methods section.

Antigen-conjugate	Supplier	Dilution
Lineage Cell Detection Mixture-Biotin, mouse	MACS Miltenyi Biotech	1:30
Streptavidin APC/Cy7	Southern Biotech	1:200
cKit-APC	eBioscience	1:200
Sca1-PerCp-Cy5.5	Biolegend	1:200
CD48-PE-Dazzle 594	Biolegend	1:200
CD48-FITC	BD Biosciences	1:200
CD135-PE	Biolegend	1:200
CD150-PE-Cy7	Biolegend	1:200
CD16/32-PE-Cy7	eBioscience	1:200
CD34-FITC	eBioscience	1:200
CD45.1(Ly5.1)-EF450	eBioscience	1:200
CD45.2(Ly5.2)-PE	Biolegend	1:200
CD45.1(Ly5.1)-PE	BD Biosciences	1:200
CD45.2(Ly5.2)-PE-Cy7	Biolegend	1:200
CD3-FITC	Biolegend	1:200
CD19-APC	BD Biosciences	1:200
Gr1-APC-Cy7	Biolegend	1:200
CD11b-PerCp-Cy5.5	BD Biosciences	1:200
CD4-APC	Biolegend	1:200
CD8a-PerCp-C5.5	BD Biosciences	1:200
CD19-APC-H7	BD Biosciences	1:200
CD43 (Ly-48) MicroBeads, mouse	MACS Miltenyi Biotech	n.a.
CD43-biotin (clone S7, RUO)	BD Biosciences	1:100
CD19-APC	Biolegend	1:200
B220-Pacific Blue	BD Biosciences	1:200
CD45.2-FITC	BD Biosciences	1:200
γH2AX	Millipore	1:1000
53BP1	Novus Biologicals	1:500
USP15 Mab ab56900	Abcam	1:500
USP15 Rb ab71713	Abcam	1:500
FUS – NB100-565	Novus Biologicals	1:500

Tubulin	Sigma	1:10,000
Goat anti-mouse HRP	Life technologies	1:10,000
Rabbit IgG 2729S	Cell Signaling Technology	
Alexa Fluor 568 goat anti-mouse	Life Technologies	1:250
Alexa Fluor 488 goat anti-rabbit	Life Technologies	1:250

Table S7. Inflammation in *Usp15*^{-/-} mice, Related to Figure 3 and Figure S4.

Genotype	Age	Cases	Sign of inflammation
<i>Usp15</i> ^{+/+}	10-12 wks	0/6	No lesions detected
<i>Usp15</i> ^{-/-}	10-12 wks	3/5	<p><i>Case 1:</i> Peritonitis, Laryngitis. Skin: Local purulent inflammatory lesions subcutaneously, showing massive infiltration of neutrophils accompanied by necrosis of the tissue. Testicular: degeneration in parts of the testes, accompanied by severe inflammatory changes in the surrounding adipose tissues with adiponecrosis. GI tract: Purulent inflammatory lesions in the mesentery accompanied by fibrosis and adherence. Spleen: Enhancement of haematopoiesis in the red pulp. Pancreas: Edematous changes with inflammatory infiltrations in stroma. Kidney: Purulent inflammatory lesions in the renal capsules and in the surrounding adipose tissues. Gall bladder: Edematous changes in the submucosa with inflammatory lesions in the surroundings. Head: Edema and inflammatory infiltrations in the submucosa of larynx. Spleen: Enhancement of hematopoiesis in the red pulp of spleen</p> <p><i>Case 2:</i> Head: -Local purulent inflammatory lesions in the skin of lip. - Otitis media in one of the middle ears. -Uterus/ovary Edematous changes of the endometrial stroma.</p> <p><i>Case 3:</i> Head: Lesions of otitis media in one of the middle ears.</p>

Histopathological analysis of *Usp15*^{-/-} mice. Full pathological analysis was performed on 6 *Usp15*^{+/+} and 5 *Usp15*^{-/-} mice between 10 and 12 weeks (wks) of age. GI: gastro intestinal tract.

Table S8. TCGA Pan-Cancer (PANCAN) samples, related to Figure 5A, B and D.

PANCAN EXPRESSION analysis (A,B)		PANCAN survival analysis (C)	
acute myeloid leukemia	173	acute myeloid leukemia	161
adrenocortical cancer	79	adrenocortical cancer	79
bladder urothelial carcinoma	427	bladder urothelial carcinoma	426
brain lower grade glioma	530	brain lower grade glioma	528
breast invasive carcinoma	1218	breast invasive carcinoma	1214
cervical & endocervical cancer	310	cervical & endocervical cancer	309
cholangiocarcinoma	45	cholangiocarcinoma	45
colon adenocarcinoma	495	colon adenocarcinoma	491
diffuse large B-cell lymphoma	48	diffuse large B-cell lymphoma	48
esophageal carcinoma	196	esophageal carcinoma	196
glioblastoma multiforme	172	glioblastoma multiforme	166
head & neck squamous cell carcinoma	566	head & neck squamous cell carcinoma	565
kidney chromophobe	91	kidney chromophobe	89
kidney clear cell carcinoma	606	kidney clear cell carcinoma	606
kidney papillary cell carcinoma	323	kidney papillary cell carcinoma	322
liver hepatocellular carcinoma	423	liver hepatocellular carcinoma	422
lung adenocarcinoma	576	lung adenocarcinoma	567
lung squamous cell carcinoma	553	lung squamous cell carcinoma	546
mesothelioma	87	mesothelioma	86
ovarian serous cystadenocarcinoma	308	ovarian serous cystadenocarcinoma	307
pancreatic adenocarcinoma	183	pancreatic adenocarcinoma	183
pheochromocytoma & paraganglioma	187	pheochromocytoma & paraganglioma	187
prostate adenocarcinoma	550	prostate adenocarcinoma	550
rectum adenocarcinoma	171	rectum adenocarcinoma	170
sarcoma	265	sarcoma	265
skin cutaneous melanoma	474	skin cutaneous melanoma	458
stomach adenocarcinoma	450	stomach adenocarcinoma	443
testicular germ cell tumor	156	testicular germ cell tumor	139
thymoma	122	thymoma	121
thyroid carcinoma	572	thyroid carcinoma	572
uterine carcinosarcoma	57	uterine carcinosarcoma	57
uterine corpus endometrioid carcinoma	567	uterine corpus endometrioid carcinoma	553
uveal melanoma	80	uveal melanoma	80
Total number of samples	11060		10951